Trapped antihydrogen

**E. Butler · G. B. Andresen · M. D. Ashkezari · M. Baquero-Ruiz · W. Bertsche ·
P. D. Bowe · C. L. Cesar · S. Chapman · M. Charlton · A. Deller · S. Eriksson ·
J. Fajans · T. Friesen · M. C. Fujiwara · D. R. Gill · A. Gutierrez · J. S. Hangst ·
W. N. Hardy · M. E. Hayden · A. J. Humphries · R. Hydomako · M. J. Jenkins ·
S. Jonsell · L. V. Jørgensen · S. L. Kemp · L. Kurchaninov · N. Madsen ·
S. Menary · P. Nolan · K. Olchanski · A. Olin · A. Povilus · P. Pusa ·
C. Ø. Rasmussen · F. Robicheaux · E. Sarid · S. Seif el Nasr · D. M. Silveira ·
C. So · J. W. Storey · R. I. Thompson · D. P. van der Werf · J. S. Wurtele ·
Y. Yamazaki · ALPHA Collaboration**

E. Butler (✉) · S. L. Kemp
Physics Department, CERN, 1211 Geneva 23, Switzerland
e-mail: eoin.butler@cern.ch

E. Butler · W. Bertsche · M. Charlton · A. Deller · S. Eriksson · A. J. Humphries ·
M. J. Jenkins · L. V. Jørgensen · N. Madsen · D. P. van der Werf
Department of Physics, Swansea University, Swansea SA2 8PP, UK

G. B. Andresen · P. D. Bowe · J. S. Hangst · C. Ø. Rasmussen
Department of Physics and Astronomy, Aarhus University, 8000 Aarhus C, Denmark

M. D. Ashkezari · M. E. Hayden
Department of Physics, Simon Fraser University, Burnaby BC, V5A 1S6, Canada

M. Baquero-Ruiz · S. Chapman · J. Fajans · A. Povilus · C. So · J. S. Wurtele
Department of Physics, University of California, Berkeley, CA 94720-7300, USA

C. L. Cesar
Instituto de Física, Universidade Federal do Rio de Janeiro, Rio de Janeiro 21941-972, Brazil

J. Fajans · J. S. Wurtele
Lawrence Berkeley National Laboratory, Berkeley, CA 94720, USA

T. Friesen · M. C. Fujiwara · R. Hydomako · R. I. Thompson
Department of Physics and Astronomy, University of Calgary, Calgary AB, T2N 1N4, Canada

M. C. Fujiwara · D. R. Gill · L. Kurchaninov · K. Olchanski · A. Olin · J. W. Storey
TRIUMF, 4004 Wesbrook Mall, Vancouver BC, V6T 2A3, Canada

A. Gutierrez · W. N. Hardy · S. Seif el Nasr
Department of Physics and Astronomy, University of British Columbia,
Vancouver BC, V6T 1Z4, Canada

Abstract Precision spectroscopic comparison of hydrogen and antihydrogen holds the promise of a sensitive test of the Charge-Parity-Time theorem and matter-antimatter equivalence. The clearest path towards realising this goal is to hold a sample of antihydrogen in an atomic trap for interrogation by electromagnetic radiation. Achieving this poses a huge experimental challenge, as state-of-the-art magnetic-minimum atom traps have well depths of only ~1 T (~0.5 K for ground state antihydrogen atoms). The atoms annihilate on contact with matter and must be 'born' inside the magnetic trap with low kinetic energies. At the ALPHA experiment, antihydrogen atoms are produced from antiprotons and positrons stored in the form of non-neutral plasmas, where the typical electrostatic potential energy per particle is on the order of electronvolts, more than 10^4 times the maximum trappable kinetic energy. In November 2010, ALPHA published the observation of 38 antiproton annihilations due to antihydrogen atoms that had been trapped for at least 172 ms and then released—the first instance of a purely antimatter atomic system confined for any length of time (Andresen et al., Nature 468:673, 2010). We present a description of the main components of the ALPHA traps and detectors that were key to realising this result. We discuss how the antihydrogen atoms were identified and how they were discriminated from the background processes. Since

S. Jonsell
Department of Physics, Stockholm University, 10691, Stockholm, Sweden

S. Menary
Department of Physics and Astronomy, York University, Toronto, ON, M3J 1P3, Canada

P. Nolan · P. Pusa
Department of Physics, University of Liverpool, Liverpool L69 7ZE, UK

F. Robicheaux
Department of Physics, Auburn University, Auburn, AL 36849-5311, USA

E. Sarid
Department of Physics, NRCN-Nuclear Research Center Negev, Beer Sheva, 84190, Israel

D. M. Silveira · Y. Yamazaki
Atomic Physics Laboratory, RIKEN Advanced Science Institute,
Wako, Saitama 351-0198, Japan

D. M. Silveira · Y. Yamazaki
Graduate School of Arts and Sciences, University of Tokyo, Tokyo 153-8902, Japan

Present Address:
L. V. Jørgensen · S. Seif el Nasr
Physics Department, CERN, 1211 Geneva 23, Switzerland

Present Address:
S. L. Kemp
Department of Physics, Durham University, Durham DH1 3LE, UK

Present Address:
J. W. Storey
Physik-Institut, Zurich University, 8057 Zurich, Switzerland

the results published in Andresen et al. (Nature 468:673, 2010), refinements in the antihydrogen production technique have allowed many more antihydrogen atoms to be trapped, and held for much longer times. We have identified antihydrogen atoms that have been trapped for at least 1,000 s in the apparatus (Andresen et al., Nature Physics 7:558, 2011). This is more than sufficient time to interrogate the atoms spectroscopically, as well as to ensure that they have relaxed to their ground state.

1 Introduction

Antihydrogen, as the bound state of an antiproton and a positron, is the simplest pure-antimatter atomic system. Hydrogen, the matter equivalent, is perhaps the best understood atomic system, with the 1S–2S atomic transition measured to a precision of 1.8 parts in 10^{14} [3], and the ground-state hyperfine splitting determined to approximately 1 part in 10^{12} [4]. This extremely high precision means that comparisons of transition frequencies in antihydrogen with those in hydrogen hold the promise of sensitive tests of CPT symmetry and matter-antimatter equivalence.

The first cold (indeed, non-relativistic) antihydrogen atoms were synthesised by the ATHENA experiment working at the CERN AD in 2002 [5]. The atoms were produced by merging cryogenic plasmas of antiprotons and positrons in a Penning–Malmberg trap. The atoms, being neutral, were not confined by the electric and magnetic fields that confine the charged particles and escaped the trap to annihilate on the surrounding apparatus. ATHENA identified antihydrogen atoms by detecting the spatially- and temporally- coincident annihilations of a positron and an antiproton at the inner surface of the trap electrodes, the first matter object encountered by an antihydrogen atom leaving the Penning–Malmberg trap. Later that year, antihydrogen was also produced and detected by the ATRAP experiment, also at the CERN AD, using a different detection technique, in which an electric field was used to field-ionise highly excited antihydrogen atoms in flight and collect the antiprotons for later counting [6].

Even though produced in cryogenic conditions, the atoms in these experiments had sufficient velocity to cross the trap in a small fraction of a second and so are short-lived and difficult to study spectroscopically. A likely better route to achieve this is to confine antihydrogen atoms in an atomic trap, where they can be held and experimented upon for a longer time. This also ensures that the highly-excited atoms thought to be produced in antiproton-positron mixing have sufficient time to reach the ground state, and could allow the application of techniques such as laser cooling to reduce the sample temperature and increase the measurement precision.

2 The ALPHA apparatus

Antihydrogen atoms do not exist in nature and thus cannot be readily loaded into an atomic trap in the usual fashion for cold-atom experiments. Instead, the atoms
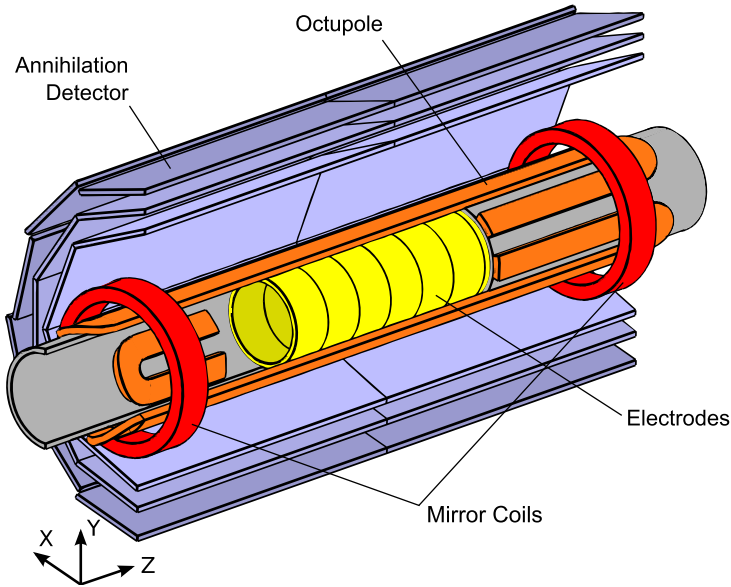
Fig. 1 A schematic, cut-away, diagram of the antihydrogen production and trapping region of the ALPHA apparatus, showing the positions of the annihilation detector, magnetic minimum trap magnets and Penning trap electrodes. The components are not drawn to scale

must be produced from antiproton-positron combination inside the atomic trap, and be prevented from reaching the trap boundaries at all times i.e. they must be 'born trapped'. A suitable geometry to achieve this is a superposition of a Penning–Malmberg trap for the charged particles and a Ioffe-type magnetic minimum trap for the neutral atoms. A schematic of this arrangement in ALPHA is shown in Fig. 1.

2.1 The magnetic minimum trap

Hydrogen (and antihydrogen) atoms have a small permanent magnetic dipole moment which, in the presence of a magnetic field, has a an associated potential energy

$$U = -\boldsymbol{\mu} \cdot \mathbf{B}. \tag{1}$$

A three-dimensional maximum of magnetic field is forbidden by Maxwell's equations, though a three-dimensional minimum is not, allowing traps for atoms with a negative $\boldsymbol{\mu}$ (so-called 'low-field-seeking atoms') to be constructed.

A common variety of magnetic minimum trap is the Ioffe–Pritchard type [7], comprised of a multipole magnet to produce a magnetic field with a minimum in magnitude transverse the axis of trap, and two short solenoids ('mirror coils') to generate a magnetic minimum along the axis. The transverse magnetic field of the multipole coil can potentially disrupt the confinement of the charged particles by the Penning–Malmberg trap. Measurements on stored non-neutral plasmas in such a device demonstrated that there is an increased rate of diffusion in the transverse direction [8], which reduces the storage time and can also result in heating through

the release of electrostatic potential energy. It is therefore desirable to reduce, as much as possible, the strength of the transverse magnetic field to which the plasmas are exposed. As the plasmas are confined in a small region near the axis of the trap, this can be achieved by choosing a higher order multipole (for a multipole of order l, the transverse magnetic field $B_\perp$ scales as r^{l-1}).

For this reason, ALPHA opted to construct an octupole-based magnetic trap instead of the more typical quadrupole-based Ioffe trap. The ALPHA octupole produces a transverse magnetic field of 1.54 T at the inner radius of the trap electrodes $r = r_w = 22.275$ mm. The centres of the mirror coil magnets are displaced 137 mm axially to either side of the trap centre, and produce a magnetic field of 1.0 T at their centres. These fields combine with a solenoidal (axial) magnetic field of 1.0 T, needed to confine particles in the Penning–Malmberg trap, to produce a trap depth of 0.8 T, equivalent to a kinetic energy of 0.54 K $\times k_B$ for ground state antihydrogen atoms.

The octupolar magnetic field increases rapidly with radial position near the current-carrying windings, so to maximise the use of the magnetic field, the distance between the windings and the inner boundary of the trap volume must be made as small as possible. For this reason, ALPHA designed the Penning–Malmberg trap electrodes in the trapping region to have a maximum thickness of less than 1 mm and wound the superconducting wire of the octupole directly onto the wall of the vacuum chamber containing the electrodes and particles.

The prototypical antihydrogen trapping experiment involves capturing antihydrogen atoms formed in the trap and later releasing these atoms by de-energising the magnets and detecting their annihilation when they strike the surrounding matter objects. In such an experiment, a large part of the background will stem from cosmic-ray particles, which can produce a false signal in the detector used to detect the annihilation products (see Section 2.2). The simplest way to reduce this background is to minimise the length of the time window over which the antihydrogen atoms are expected to escape. This is accomplished using the 'quench protection system' of the magnets; a similar system is present in many powered superconducting magnets to protect the magnet from any damage that could be caused by run-away heating due to a transition from the superconducting to normally-conducting state in the magnet system (a 'quench'). In ALPHA, a system of voltage monitors detects a quench through the voltage drop induced by current flowing in a section of normally conducting material [9]. In an antihydrogen trapping experiment, the quench protection system is deliberately externally triggered to induce the rapid shutdown of the trap.

A semiconductor switch (of the IGBT type) is used to rapidly divert the current flowing in the magnets through an external resistor network, where the energy is dissipated as heat. Simultaneously, current entering from the power supply is diverted using a second semiconductor device. The speed at which the current is removed is determined by the inductance of the magnet and the resistance of external resistor network, and is limited by the maximum voltage that is safe to induce across the magnet. Measurements of the current decay (Fig. 2) show that the currents decay with time constants 9 ms in the octupole and 8 ms in the mirror coils. We define an observation window of 30 ms following the shutdown over which we expect antihydrogen atoms to escape. The short length of this window reduces, by a large factor, the level of background from cosmic rays.

Fig. 2 The measured current
flowing in the magnetic
minimum trap magnets
following a triggered shutdown
at $t = 0$. The dependence is
exponential, with time
constants 9 ms for the octupole
and 8 ms for each of the mirror
coils. The *shaded* region shows
the 30 ms window over which
the search for the escape of
trapped antihydrogen atoms
was conducted
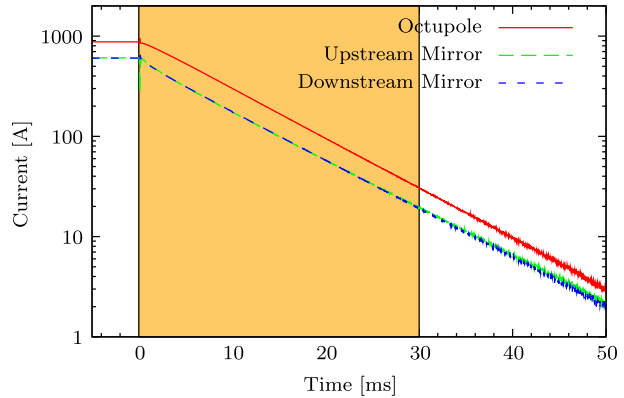
2.2 Antiproton annihilation detector

An antiproton escaping the trap will impact, and annihilate upon, the inner surface
of the Penning–Malmberg trap electrodes. An antiproton annihilation will produce
a number of charged particles that will penetrate the surrounding material. The
ALPHA detector is a three-layer, two-sided silicon strip detector designed to track
the daughter particles and identify their common point of origin to determine the
three-dimensional position of the antiproton's annihilation. The detector extends
over the entire trapping region and has a total active length of 46 cm.

Passage of the charged particles through the silicon leaves charge deposits ('hits'),
which are amplified and digitised to determine the three-dimensional point of
passage. Determining the particles' trajectories becomes a sophisticated game of
'join-the-dots', and the intersection of the trajectories ('tracks') determines the point
of annihilation ('vertex'). Example of reconstructed events can be seen in Fig. 3,
while further details of the algorithm can be found in [10]. The detector can resolve
annihilations with a precision of approximately 0.27 cm in the axial direction and
0.44 cm in the transverse direction.

High-energy particles from cosmic rays that pass through the detector can appear
to be composed of two almost-collinear tracks. Such events can be mistaken for
antiproton annihilations, and form one of the principal backgrounds to identifying
trapped antihydrogen atoms. To distinguish cosmic-rays, and eliminate them as sig-
nal, we define criteria on a number of parameters of the reconstructed annihilation.
We expect antiproton annihilations to occur within the Penning–Malmberg trap (i.e.
within 2.2 cm of the axis of the experiment), while cosmic rays can be scattered
through the detector volume, so we require that the distance from the axis is less
than 4 cm. In addition, we fit a straight line to sets of six charged particle hits and
examine the sum of the squared residual distances. Cosmic rays tend to resemble
straight lines and are characterised by small values of this quantity. When there are
just two identified tracks, we require the residual to be greater than 2 cm^2. When
there are more than two identified tracks, we can relax this criteria, as only rarely do
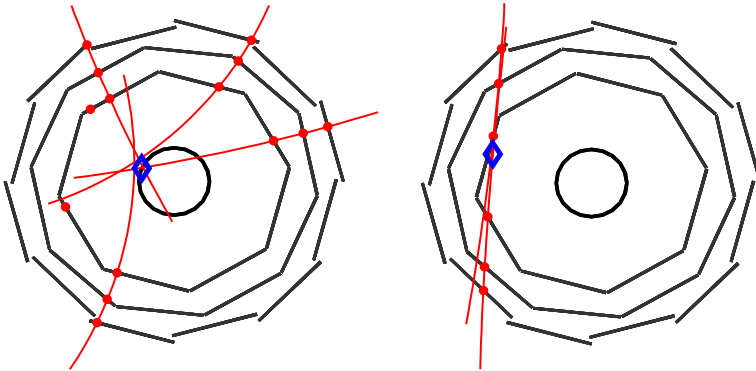cosmic rays produce more than one track; we require the squared residual value to
exceed 0.05 cm^2.

Fig. 3 Examples of a typical antiproton annihilation and cosmic ray event as reconstructed by the ALPHA detector. The *straight* segments are the silicon layers, the *circle* is the inner radius of the Penning–Malmberg trap electrodes, the *red points* mark charged-particle hits, the *red curved lines* are reconstructed tracks, and the *blue diamond* is the position of the reconstructed vertex

Using this method, we reduce the background acceptance rate to $(47 \pm 2) \times 10^{-3}$ s^{-1} (from a 'raw' trigger rate of $\sim$10 s^{-1}), while retaining $\sim$64% of annihilations [2].

3 Producing trappable antihydrogen

A simple model for the number of antihydrogen atoms that can be trapped can be expressed as the following equation:

$$N_{\text{trapped}} = N_{\text{produced}} \times f_{\text{LFS}} \times f_{0.54 \text{ K}}, \tag{2}$$

where N_{trapped} and N_{produced} are the number of antihydrogen atoms trapped and produced, respectively, f_{LFS} is the fraction of atoms produced in trappable, low-field-seeking, states and $f_{0.54 \text{ K}}$ is the fraction of atoms that are produced with an energy below 0.54 K.

The number of antihydrogen atoms produced in an experiment depends on a large number of variables, including the numbers, density, and temperatures of positrons and antiprotons present, the electric and magnetic fields present, etc... and is not easily calculable, but is rather better measured.

The fraction of atoms in low-field seeking states is a function of the temperature of the positron plasmas [11]. At the temperatures typical in ALPHA (50–100 K), to a good approximation, half of the atoms will be low-field-seeking [11].

Antihydrogen atoms are produced by confining spatially overlapping distributions of antiprotons and positrons in a nested Penning trap (see Fig. 4), [12]. A positron plasma is placed at the centre of the nested well, while antiprotons in an excited distribution pass back and forth, interacting with the positron plasma, with some fraction combining to produce antihydrogen. Due to the larger mass of the antiprotons, the momentum of an antihydrogen atom produced will be dominated by the momentum of the antiproton immediately before combination. This can be thought of as being made up of 'thermal' motion in a random direction characterised by a continuous
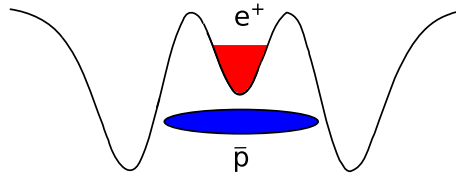
Fig. 4 A schematic representation of a nested Penning trap, showing the electric potential as a function of the axial coordinate. In this example, positrons (e^+) are held in the central well, while antiprotons ($\bar{p}$) are confined in the outer well

velocity distribution and an additional 'E × B' component due to the forces on the antiproton by the electric and magnetic fields in the trap. The value of $f_{0.54\,K}$ is determined by integrating the velocity distribution defined by these components up to the trap depth.

3.1 Autoresonant injection

Measurements by the ATHENA collaboration [13] indicated that when antiprotons were introduced ('injected') with several eV of kinetic energy, the resulting antihydrogen velocity distribution had a non-isotropic character, indicating that antihydrogen formation occurred before the antiprotons and positrons had come into equilibrium. In this case, it is likely that the antihydrogen had velocities commensurate with a substantial fraction of the several-electronvolt injection energy.

To minimise this effect, ALPHA developed an alternative technique to produce an antiproton distribution that allowed the antiprotons and positrons to be placed in contact with lower relative kinetic energies. This technique relies on the autoresonant excitation of the axial oscillatory motion of the antiproton cloud [14]. When antiprotons are placed in an anharmonic potential such as that found in the 'sidewells' of the nested Penning trap, the position of the centre-of-charge of the cloud exhibits oscillatory behaviour with a frequency that is a function of the longitudinal energy. It is a general property of such oscillators that when the frequency of an external resonant drive is changed, that the oscillator's energy will change to keep the oscillatory motion in resonance with the drive.

As the frequency of the external drive can be well-controlled, this allows for precise control of the longitudinal energy of the antiprotons. When used as an injection tool, one makes use of the fact that the longitudinal energy-oscillation frequency relationship has a discontinuity when the antiprotons have just enough energy to enter the positron plasma. When driven to this point, antiprotons fall out of resonance with the drive and cease to resonantly gain energy. This can be exploited to inject antiprotons into the positron plasma with a minimum of relative kinetic energy.

Autoresonance is quite a general phenomenon: it has been observed and has found applications in several areas of physics, including particle accelerators, the motion of celestial bodies, and trapped non-neutral plasma modes. The specific application of autoresonance to excitation of antiproton plasmas in ALPHA can be found in [14–16].

3.2 Evaporative cooling

In a low-relative kinetic energy arrangement such as that produced by autoresonant injection, calculations and preliminary measurements indicate that the antiprotons and positrons will come into equilibrium quickly, and the thermal component of the antiproton/antihydrogen velocity will be characterised by the temperature of the positron plasma [11, 17]. In the parameter range in which ALPHA typically operates (where the positron temperature is 50–100 K, the positron density is $\sim 7 \times 10^7$ cm^{-3}, and the typical antiproton radius is 0.4 mm), the thermal component of the velocity ~ 500 m s^{-1} dominates over the E $\times$ B component (~ 200 m s^{-1}), and thus is the principal determining factor for the fraction of antihydrogen atoms that can be trapped. Reduction in the positron temperature, all else remaining equal, will thus be expected to increase the number of trapped antihydrogen atoms. At sufficiently low positron temperatures, the E $\times$ B contribution will become dominant, and the route towards higher numbers of trapped antihydrogen atoms will be, all else being equal, through reducing the electric field (by reducing the positron plasma density) or through compressing the antiproton cloud closer to the trap axis.

As passive cooling through the emission of cyclotron radiation appears to be unable, by itself, to cool stored plasmas in ALPHA to very low temperatures, active cooling techniques must be employed to produce colder plasmas. To achieve this, ALPHA has adopted a technique from atomic physics—evaporative cooling. On neutral atoms, evaporative cooling has been key to preparing ultra-cold ensembles of atoms and achieving Bose–Einstein condensation [18]. Before demonstrated by ALPHA [19], evaporative cooling of charged particles at cryogenic temperatures had never been achieved.

The principle of evaporative cooling is the selective removal of particles from the high-energy tail of a velocity distribution. When the hottest particles are removed, the mean energy per remaining particle is reduced, and the distribution evolves through collisions and reaches an equilibrium at a lower temperature. In charged-particle evaporative cooling in a Penning–Malmberg trap, the high-energy particles are removed by placing the plasma in a shallow potential well. The energy of any particle fluctuates as it undergoes collisions with other particles; a particle that reaches an energy larger than the well depth U will simply pass over the confining potential and escape the trap. We characterise the temperature of a plasma stored in this regime by the ratio of well depth to temperature $\eta = U/k_B T$ and the evaporation rate by a evaporation time τ_{ev}, defined by $dN/dt = N/\tau_{ev}$, where N is the number of particles. τ_{ev} can be related to η and the antiproton-antiproton collision rate τ_{col} through [19]

$$\frac{\tau_{ev}}{\tau_{col}} = \frac{2}{3} \eta \, e^{\eta}. \tag{3}$$

The exponential dependence of τ_{ev} on η means the evaporation rate drops precipitously once η becomes low enough, with the result that, to a good approximation, T is a function of only U (i.e. η tends to a constant value). For evaporative cooling on antiprotons, we have found that in the range $\sim 10 - 1,000$ K, η is approximately constant, with a value ~ 12.

Evaporative cooling inherently involves sacrificing some of the stored particles, reducing the density of particles in the trap, and there is a trade-off between

achieving lower temperatures and retaining a larger fraction of particles. Typically, we employ evaporative cooling on antiprotons to temperatures of 100–200 K, which retains approximately 50% of the particles when starting from a temperature of ∼600 K. We have achieved antiproton temperatures as low as (9 ± 4) K, while retaining as much as 10% of the starting number of particles.

The particles evaporating from the plasma are lost close to the axis of the trap, where the well depth is smallest. This creates a hollowed-out charge profile, which tends to redistribute itself to an equilibrium shape. In doing so, the total canonical angular momentum of the particles must be conserved, and thus the plasma expands transversely. For particles escaping exactly on the axis (in reality, they escape from an area approximately one Debye length across), the size of the plasma will follow [19]

$$\frac{r}{r_0} = \sqrt{\frac{N_0}{N}}, \tag{4}$$

where r and N are the plasma radius and number of particles, respectively, and the subscript zero refers to the initial conditions. Transverse expansion is undesirable, as it increases the magnitude of the E × B velocity when the antiprotons pass through the positron plasma.

Evaporative cooling can also be employed on plasmas of electrons and positrons. Indeed, since antihydrogen is formed at the positron temperature, evaporative cooling of positrons has a more direct impact on the number of trappable antihydrogen atoms produced than cooling of the antiprotons. The behaviour of evaporative cooling on the lighter species is qualitatively the same as for antiprotons, except that the timescales are much shorter, as might be expected from the high collision and cyclotron radiation rates. Further details on evaporative cooling in ALPHA can be found in [19] and [20].

4 Identifying trapped antihydrogen

As already described, detection of trapped antihydrogen in ALPHA involves switching off the magnetic trap and identifying the annihilation of antihydrogen atoms as they impact the apparatus. There are two principal types of backgrounds to consider. The first is comprised of non-annihilation events recorded by the annihilation detector, mostly made up of cosmic rays and electronic noise. These processes have an approximately constant rate, and are suppressed by the short trap shut-off time and effectively eliminated by examination of the event topology, leaving a background rate of only 47 mHz (Section 2.2). The second background process is made up of real antiproton annihilations that are not due to antihydrogen atoms, most likely due to rare antiprotons that can become trapped in the magnetic minimum. Such antiprotons produce identical annihilation signals to bare antiprotons, and present a background for trapped antihydrogen detection.

Charged particles in a magnetic field with spatially-varying strength move in an effective potential

$$V = E_{\perp,0} \left(\frac{B - B_0}{B_0} \right) + q\,\Phi, \tag{5}$$

where $E_{\perp,0}$ is the kinetic energy of the particles in the degrees of freedom transverse to the magnetic field at the point where $B = B_0$, q is the charge of the particle and Φ is the electric potential. Both B and Φ can be spatially varying. Particles trapped in spatially varying magnetic fields are usually referred to as 'mirror-trapped'.

To remove such particles, ALPHA applies a series of spatially and temporally-varying electric field pulses so that, for all particles with $E_{\perp,0} \lesssim 25$ eV, no minimum of the effective potential exists and the particles are removed. In the complicated three dimensional field configuration, the motion of the antiprotons and the probability that they are removed from the trap by the electric fields are evalued by a Monte-Carlo like computer simulation, incorporating realistic models of the experiment geometry. However, the simulations imply that particles with higher $E_{\perp,0}$ could still be trapped.

Obvious potential sources of high $E_{\perp,0}$ antiprotons (such as antihydrogen field-ionsation, antiproton-gas collisions, etc...) have been considered and the rates at which they occur have be calculated to be too small to contribute to a signal [11]. However, given that there are many complex factors at play, and that there was such a large disparity between the number of antiprotons present in the apparatus during antihydrogen production, just prior to the trapped-atom identification window, and the sensitivity to trapped antihydrogen ($\sim$30,000 antiprotons versus $\lesssim$0.1 atoms per trial), it was difficult to guarantee that deficiencies in the model of the experiment or unaccounted-for processes cannot contribute at the level of 1 part in 10^{-5}.

It is possible to distinguish between trapped antihydrogen atoms and mirror-trapped antiprotons by examining the position and time at which the particles escape the magnetic trap. Uncombined antiprotons and neutral antihydrogen atoms are expected to produce different distributions in the two-dimensional (z, t) parameter space of the annihilation, mostly due to the differing scale of their velocities compared to the timescale at which the magnetic field is removed. Antihydrogen atoms with 0.54 K of kinetic energy move at less than 100 m s^{-1}, and take of order 1 ms to cross the trap, while electronvolt range antiprotons have velocities in the range 10^4 m s^{-1} and cross the trap in no more than tens of microseconds. Antiprotons thus have time to 'explore' the trap boundaries and are more likely to escape the trap close to the point where the trap depth is lowest, which is midway between the mirror coils. The magnetic field changes substantially over one period of an antihydrogen atom's motion in the trap, and therefore the escape positions will be more widely spread around the central position.

The exact escape distributions can be calculated with extensions of the computer simulations mentioned above, incorporating measurements of the decay of the current in the magnets, and compared to the positions of observed annihilation events, measured using the annihilation imaging detector, to evaluate if the event is compatible with the escape of an antihydrogen atom (signal) or a bare antiproton (background). Figure 5a shows the simulated (z, t) distribution for antihydrogen atoms as grey points, while the distribution for antiprotons escaping in a flat electric potential can be seen as the green points in Fig. 5b.

During 2009, ALPHA conducted an antihydrogen trapping experiment, during which six 'candidate' events (i.e. fulfilling the criteria for selection as an annihilation-like event) were identified [11]. The expected background from falsely selecting cosmic-ray events as annihilations was 0.14 events, meaning that the observation of six events had a significance of 5.6σ above the background. While a comparison
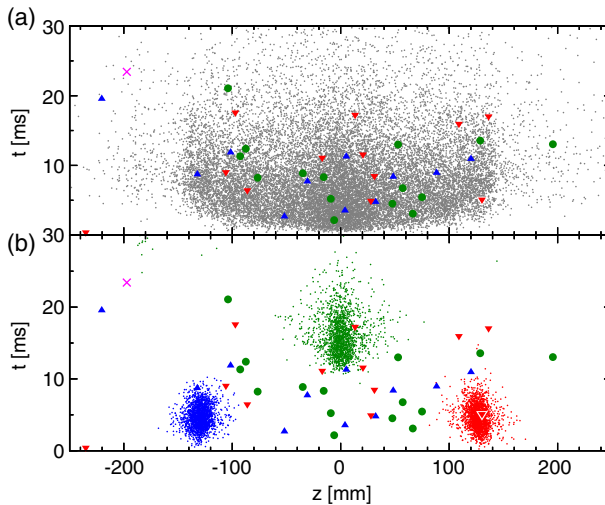
Fig. 5 The two-dimensional time-position (z, t) distributions for the escape positions of (**a**) antihydrogen atoms and (**b**) mirror-trapped antiprotons after a shutdown of the magnetic trap at $t = 0$. The *dots* are the result of numerical simulations of the trajectories of the particles in the magnetic and electric fields of the apparatus. In (**b**), the *green*, *blue* and *red* distributions correspond to experiments with no applied electric field, an electric field pointing to positive z and an electric field pointing to negative z respectively. The *green circles*, *blue up-pointing triangles* and *red down-pointing triangles* mark the measured times and positions of candidate antihydrogen annihilations in ALPHA for the same electric field configurations. The *magenta cross* marks the position of the event observed after antihydrogen production using externally-heated positrons

of the (z, t) coordinates of the candidates and the simulated distributions implied that the events were incompatible with a mirror-trapped antiproton background, a number of unknowns, including how well the simulated experiment reflected the real device, remained and stronger discrimination was needed to definitively identify trapped antihydrogen.

Still clearer identification can be achieved by releasing the trap while applying an axial electric field. Bare antiprotons, being charged, will be deflected to one side, while the neutral antihydrogen atoms will not be affected. The blue and red coloured points in Fig. 5b show the simulated distributions for electric fields with $E_z > 0$, which pushes antiprotons to the left (negative z) and $E_z < 0$, pushing antiprotons to the right (positive z). The results of these simulations are valid up to antiproton energies at least of the order of hundreds of electronvolts, higher than any plausible mechanism related to antihydrogen production. Experiments using artificially-produced distributions with high $E_{\perp,0}$ to deliberately mirror-trap antiprotons have reproduced the behaviour of the simulations.

A final control experiment, to rule out more exotic processes that could produce very high-energy antiprotons (one possibility could be related to the capture of the antiproton beam from the Antiproton Decelerator) makes use of a radio-frequency drive to artificially heat the positron plasma during antihydrogen production [5]. This is expected to suppress the number of trapped atoms in two ways—first, the number of atoms produced will decline due to the inverse dependence of the production rate on the positron temperature. Secondly, the temperature of the

Table 1 A summary of the number of number of detector events meeting the criteria for selection as antiproton annihilations and rejection as cosmic rays in the experiments with different configurations of electric field and with heated positrons (from [1])

Experiment type	Number of attempts	Antiproton annihilations
$E_z = 0$	137	15
$E_z > 0$	101	11
$E_z < 0$	97	12
Heated positrons	246	1

atoms will be higher, and fewer will have trappable kinetic energies. In a series of 246 experiments, one annihilation signal was observed, incompatible with both the antihydrogen and antiproton escape distributions (see the magenta point in Fig. 5), and is possibly attributable to a misidentified cosmic-ray particle (the expected cosmic-ray background in 246 experiments is 0.34 events).

A series of experiments incorporating the full range of controls and check experiments was carried out at ALPHA in 2010, and is presented in full in reference [1]. The main results of this experiment can be see in Fig. 5, where the coloured circles and triangles mark the times and positions of detector events that fulfilled the criteria for selection of an antiproton annihilation. Three configurations of the electric field present during the measurement were used: none, a field to deflect antiprotons to the left, and one to deflect antiprotons to the right.

The number of experiments and observed annihilations are summarised in Table 1. The expected cosmic background for these measurements is 0.46, with which the observation of 38 annihilation-like events is incompatible to a significance level of more than 16 standard deviations. Comparing the measured events to the simulated (z, t) distributions in Fig. 5, we see that the observed annihilations are highly incompatible with the release of mirror-trapped antiprotons, and (with a few exceptions) are consistent with the expected distribution of trapped antihydrogen annihilations. In addition, the distributions measured with different applied electric potentials are consistent with each other, indicating that the trapped particles are not affected by electric fields, and are thus likely to be neutral.

This allows us to rule out the backgrounds and conclude that antihydrogen atoms had been trapped in the experiment, the first time that this had been achieved.

Continuing development and refinement of the antihydrogen production technique has resulted in improvements in the number of antihydrogen atoms trapped and detected each experiment, and rates approaching one trapped atom per trial, compared to 1 in ∼9 in [1], have been achieved. This is the most relevant parameter to experimental operations, as it will determine the size of the spectroscopic signal that can be generated in a given run period.

5 Long-time confinement of antihydrogen atoms

Without knowing how long the antihydrogen atoms produced could survive in the magnetic minimum trap, the first experiments [1] were designed so that the trap de-energised immediately after clearing away left-over antiprotons and positrons. This took place over 172 ms, setting a rough lower bound on the typical confinement time.

Table 2 Summary of number of experiments and number of detected annihilation events for various holding times

Holding time (s)	0.4	10	50	180	600	1,000	2,000
Number of experiments	119	6	13	32	12	16	3
Detected events	76	6	4	14	4	7	1

By simply inserting a pause ('holding time') between the removal of the uncombined particles and the release of the trap, we can directly measure the confinement time.

Table 2 shows the number of experiments and number of annihilation events observed with holding times between 0.4 and 2,000 s (reported in [2]). At holding times shorter than 1,000 s, the annihilations are incompatible with the cosmic background to a significance $\sim 8.0\sigma$, allowing us to draw the conclusion that some atoms survive at least this long in the apparatus.

The limiting factor is expected to be interactions between the antihydrogen atoms and residual gas atoms in the apparatus, either through collisional energy transfer imparting enough kinetic energy to the trapped atoms to drive them from the trap, or through annihilation between the antiproton and a gas nucleus [2]. The cryogenic vacuum conditions in the ALPHA apparatus (estimated at a atom/molecule density of 5×10^{10} m^{-3} for hydrogen or helium) plays a large part in reducing the rates of these processes to of the order of 1,000 s.

6 Outlook

The realisation of trapped antihydrogen opens the door to the first spectroscopic measurements on pure-antimatter atoms, and eventually leading to high-precision measurements capable of testing CPT and matter-antimatter symmetries. The long confinement time (of order 1,000 s) enables a correspondingly long interaction time between the atoms and the electromagnetic radiation. The first measurements are likely to be to probe the ground-state hyperfine structure (using microwave-frequency fields [21]), while preparations are underway to construct an apparatus that will admit laser radiation to probe the 1S–2S transition.

The challenges that must be faced include the prospect of precision spectroscopy in the presence of the highly-inhomogeneous magnetic fields, and producing a sufficiently high radiation density over a significant fraction of the large trap volume (~ 1 dl). The experiments are envisaged to use the identification of the annihilation of an atom driven from a trapped to an untrapped state as the spectroscopic signal, and identification of such annihilations against the cosmic-ray background over extended periods of time will remain important. As always, improved understanding and control over the antihydrogen production process will produce larger numbers of trapped atoms available for experimentation and will be needed to reach higher levels of spectroscopic sensitivity.

In addition to the direct impact on spectroscopic measurements, the long antihydrogen atom confinement time makes possible experiments that would have been considered impossible before. Among them is possible laser cooling, which would open the road to cooling to a level where gravitational effects would become apparent.

References

1. Andresen, G.B., et al. (ALPHA): Nature **468**, 673 (2010)
2. Andresen, G.B., et al. (ALPHA): Nature Physics **7**, 558 (2011)
3. Niering, M., et al.: Phys. Rev. Lett. **84**, 5496 (2000)
4. Hellwig, H., et al.: IEEE Trans. Instrum. Meas. **IM-19**, 200 (1970)
5. Amoretti, M., et al. (ATHENA): Nature **419**, 456 (2002)
6. Gabrielse, G., et al. (ATRAP): Phys. Rev. Lett. **89**, 233401 (2002)
7. Pritchard, D.E.: Phys. Rev. Lett. **51**, 1336 (1983)
8. Gilson, E.P., Fajans, J.: Phys. Rev. Lett. **90**, 015001 (2003)
9. Bertsche, W., et al. (ALPHA): Nucl. Instrum. Methods Phys. Res. A **566**, 746 (2006)
10. Hydomako, R.. et al. (ALPHA): Antihydrogen detection in ALPHA. (this conference)
11. Andresen, G.B., et al. (ALPHA): Phys. Lett. B **695**, 95 (2011)
12. Gabrielse, G., et al.: Phys. Lett. A **129**, 38 (1988)
13. Madsen, N., et al. (ATHENA): Phys. Rev. Lett. **94**, 033403 (2005)
14. Andresen, G.B., et al. (ALPHA): Phys. Rev. Lett. **106**, 025002 (2011)
15. Bertsche, W., et al. (ALPHA): Antihydrogen formation by autoresonant excitation of antiproton plasmas. (this conference)
16. So, C., et al. (ALPHA): Autoresonant mixing simulation in the ALPHA apparatus. (this conference)
17. Hurt, J., et al.: J. Phys. B: At. Mol. Opt. Phys. **41**, 165206 (2008)
18. Davis, K.B., et al.: Phys. Rev. Lett. **74**, 5202 (1995)
19. Andresen, G.B., et al. (ALPHA): Phys. Rev. Lett. **105**, 013003 (2010)
20. Silveria, D., et al. (ALPHA): Evaporative cooling of antiprotons and positrons for the production of trappable antihydrogen. (this conference)
21. Ashkezari, M., et al. (ALPHA): Progress towards microwave spectroscopy of trapped antihydrogen. (this conference)